JPET Fast Forward. Published on June 15, 2005 as DOI: 10.1124/jpet.105.087056

Multiple Components of 2,4-Dichlorophenoxyacetic Acid Uptake by Rat Choroid Plexus

Simon Lowes, Destiny Sykes, Christopher M. Breen, Leigh J. Ragone, David S. Miller

Laboratory of Pharmacology and Chemistry

National Institute of Environmental Health Sciences

National Institutes of Health

Research Triangle Park, NC 27709, USA

Running title: Components of 2,4-D Uptake by Choroid Plexus

Corresponding author :

Dr. David S Miller
Laboratory of Pharmacology and Chemistry
National Institute of Environmental Health Sciences
National Institutes of Health
P.O. Box 12233
Research Triangle Park, NC 27709, USA
Phone: 919 541 3235
FAX: 919 541 5737
miller@niehs.nih.gov

Number of text pages :	**26**
Number of Tables :	**0**
Number of Figures :	**12**
Number of References :	**25**
Number of words in :	
Abstract	**208**
Introduction	**746**
Discussion	**1186**

Abbreviations :

2,4-D, 2,4-dichlorophenoxyacetic acid ; aCSF, artificial cerebrospinal fluid ; DHEAS, dehydroepiandrosterone sulfate ; ES, estrone sulfate ; HIAA, 5-hydroxyindole acetic acid ; α-KG, α-ketoglutarate; Mrp, multidrug resistance-associated protein subtype ; Oat, organic anion transporter subtype; Oatp, organic anion transporting polypeptide subtype ; PAH, p-aminohippurate ; TC, taurocholate

ABSTRACT

Initial rates of uptake of the herbicide, 20 μM 2,4-dichlorophenoxyacetic acid (2,4-D), were measured in intact lateral choroid plexus from rat. Although inhibition of uptake by millimolar concentrations of estrone sulfate (ES) and unlabeled 2,4-D was maximal at 85%, inhibition by p-aminohippurate (PAH) saturated at about 50%. Inhibition by ES plus PAH was no greater than by ES or 2,4-D alone. Thus, inhibition studies indicated three distinct components of uptake; two mediated and one not. The Na-dependent component of 2,4-D uptake coincided with the PAH-sensitive component, indicating uptake mediated by Oat3. Consistent with this, efflux of 2,4-D from preloaded tissue was accelerated by all Oat3 substrates tested and 2,4-D increased the efflux of the Oat3 substrate, PAH. Consistent with the inhibition data, kinetic analysis showed three components of 2,4-D uptake: a non-mediated component (linear kinetics), a high affinity component and a low affinity component. The high affinity component appeared to coincide with the PAH-sensitive and Na-dependent component characterized in inhibition studies. The PAH-insensitive, low affinity component was inhibited by ES, DHEAS and taurocholate but not by HIAA. Thus, the first step in transport of 2,4-D from cerebrospinal fluid to blood involves two transporters: Oat3 and a PAH-insensitive, Na-independent transporter. Based on inhibitor profile, the latter may be Oatp3.

INTRODUCTION

One function of the choroid plexus is the removal from cerebrospinal fluid (CSF) to blood of potentially toxic xenobiotics, xenobiotic metabolites and waste products of normal central nervous system (CNS) metabolism. This is evident from in vivo experiments in which xenobiotics injected into the ventricles of test animals are rapidly cleared to the blood and in vitro experiments in which isolated tissue rapidly accumulates and concentrates xenobiotics added to artificial CSF (aCSF) bathing the ventricular surface (Pritchard and Miller, 1993; Ghersi-Egea and Strazielle, 2002; Kusuhara and Sugiyama, 2004). Transport from CSF to blood involves three steps: uptake from CSF at the apical plasma membrane, transit across the epithelial cell and efflux at the basolateral membrane into the subepithelial space and fenestrated capillaries. Recently, all of these steps have been visualized in living rat and mouse choroid plexus using confocal imaging of fluorescent xenobiotics (Breen et al., 2002; Sweet et al., 2002; Breen et al., 2004; Sykes et al., 2004).

Choroid plexus morphology is complex, with the apical plasma membrane of the epithelium exposed to CSF and the basolateral membrane facing blood vessels within the tissue. When isolated from the brain, choroid plexus from the lateral ventricles presents an epithelium-covered surface in which the apical plasma membrane is in direct contact with the medium. Confocal imaging studies of isolated, intact rat choroid plexus show that fluorescein, a fluorescent organic anion and Oat3 substrate, enters the cells well before the vascular space (Breen et al, 2002), indicating that immediate access is to the apical (ventricular) surface of the tissue. Thus, in vitro measurements of solute uptake over short incubation times provide a means to characterize uptake at the apical membrane, the first step in transport from CSF to blood (Miller, 2004).

Although the ability of the choroid plexus to transport organic anions has been known for some time (Pappenheimer et al., 1961), it has only been recently that the molecular basis of transport has been explored. RT-PCR studies show that mRNA for 10 multispecific organic anion transporters from the Oat, Oatp and Mrp families are expressed in the tissue (Choudhuri et al., 2003). Of these, 6 organic anion transport proteins have been localized to one side of the tissue or the other (Fig. 1) and recent attempts to functionally map transport of specific organic anions in intact tissue suggest important roles for Oat3 and Oatp3 at the apical membrane and Oatp2 and Mrp1 at the basolateral membrane (Sweet et al., 2002; Breen et al., 2004; Sykes et al., 2004). Such studies have been particularly successful in the mouse, because of the availability of transgenic animals that fail to express specific transport proteins, e.g., Mrp1-, Mrp4- and Oat3-null mice (Wijnholds et al., 2000; Sweet et al., 2002; Leggas et al., 2004; Sykes et al., 2004). However, it is also becoming increasingly clear that not all transport processes identified in intact tissue match transporters that have both been characterized in expression systems and shown to be expressed in the tissue (Breen et al., 2004; Sykes et al., 2004).

2,4-Dichlorophenoxyacetic acid (2,4-D) is an anionic herbicide handled by organic anion transport systems in kidney and choroid plexus. Previous studies have shown rapid clearance of 2,4-D from CSF in vivo and specific, concentrative and ouabain-sensitive uptake in vitro (Pritchard, 1980; Kim and O'Tuama, 1981; Pritchard et al., 1999; Villalobos et al., 2002). Using isolated apical (brush border) membrane vesicles from cow choroid plexus and intact choroid plexus from cow and rat, Pritchard et al (1999) showed that 2,4-D uptake is indirectly coupled to Na. Although these authors initially concluded that Oat1 was responsible for Na-dependent 2,4-D uptake in choroid plexus, it now appears that Oat3 not Oat1 is the primary Na-dependent organic anion transporter at the apical membrane (Nagata et al., 2002; Sweet et al., 2002; Sweet

et al., 2003; Sykes et al., 2004). Consistent with this, Nagata et al. (2004) recently found that 2,4-D was a moderately high affinity substrate in Oat3-transfected LLCPK1 cells (apparent Km 20 μM) and that the uptake kinetics and inhibitor profile in intact rat choroid plexus matched that of the transfected cells. These authors also concluded that the kinetics of 2,4-D uptake by rat choroid plexus could be described by a single, Oat3-mediated component plus diffusion. In the present study we used inhibitor profile, Na-dependence and organic anion exchange to confirm Oat3 as the transporter responsible for high affinity 2,4-D uptake. However, we also present evidence for a second, lower affinity, Na-independent component of 2,4-D uptake.

MATERIALS AND METHODS

Chemicals. ^{3}H-2,4-D (20 Ci/mmol) and ^{3}H-PAH (15 Ci/mmol) were purchased from American Radiolabeled Chemicals (St. Louis, MO). Unlabeled chemicals were obtained from commercial suppliers at the highest purity available.

Animals. Lateral choroid plexuses were isolated from adult, male Harlan Sprague-Dawley rats (250-400 g, obtained from Taconic Farms) using Dumont #5 forceps inserted into each hemisphere of the brain. Tissue was immediately transferred to ice-cold, artificial cerebrospinal fluid (aCSF: 103 mM NaCl, 4.7 mM KCl, 2.5 mM $CaCl_2$, 1.2 mM KH_2PO_4, 1.2 mM $MgSO_4$, 25 mM $NaHCO_3$, 10 mM glucose, 1 mM sodium pyruvate, at pH 7.4), previously gassed with 95% O_2/5% CO_2. Tissue was preincubated in gassed aCSF at 37º C for 15 min before transport experiments. Animal housing was in accordance with institutional guidelines and the NIH Guide for the Use and Care of Laboratory Animals.

^{3}H-2,4-D Transport. For uptake measurements, each lateral choroid plexus (about 1 mg) was incubated with shaking at 37º C in 1 ml continuously gassed (95% O_2/5% CO_2) aCSF containing ^{3}H-2,4-D, unlabeled 2,4-D and the indicated additions. After incubation, tissue was removed, rinsed briefly, weighed and processed for liquid scintillation counting. Tissue accumulation of 2,4-D was calculated from dpm/mg tissue wet weight and medium specific activity. In some experiments, tissue was incubated in Na-free aCSF, with NaCl and $NaHCO_3$ replaced with cholineCl and cholineHCO_3, respectively. Initial experiments indicated no loss of viability (preserved morphology and ability to concentrate organic anions) when tissue was incubated in gassed aCSF for periods up to 90 min.

For efflux measurements, tissue was loaded by incubation for 30 min at 37º C in continuously gassed (95% O_2/5% CO_2) aCSF containing 20 μM ^{3}H-2,4-D. Each plexus was then briefly washed and transferred to 1.5 ml gassed (95% O_2/5% CO_2) aCSF without (control) or with unlabeled compounds. Vials were shaken and continuously gassed. At preset intervals, 50 μl of efflux medium was taken for liquid scintillation counting. After 60 min, a final medium sample was taken and the tissue and all medium samples were removed and processed for liquid scintillation counting. Total tissue dpm at the beginning of the efflux period was calculated from final tissue dpm and final medium dpm plus dpm removed for the timed samples. At each sampling time, the fraction of total label remaining in the tissue was calculated from initial total tissue dpm and medium dpm at the sampling time (corrected for dpm removed in previous samples).

Statistics. Data are presented as mean ± SE. Means were compared using Student's t test or one-way ANOVA. Means were deemed to be significantly different when $P < 0.05$. Linear and non-linear regression analyses were carried out using GraphPad Prism 4.0 software.

RESULTS

Inhibition of 2,4-D Uptake. Recent studies have provided a functional characterization of Oat1 and Oat3, the only two transporters known to be capable of concentrative, Na-dependent organic anion uptake. When cloned rat, mouse and human transporters were expressed in xenopus oocytes, they were shown to be organic anion-dicarboxylate exchangers (Sweet et al., 2003). For each species, Oat1 and Oat3 could be differentiated based on substrate and inhibitor specificity: PAH was a substrate and inhibitor of both, but estrone sulfate (ES) interacted with Oat3, not Oat1. Transport data from kidney and choroid plexus of Oat3-null mice confirmed this dichotomy (Sweet et al., 2002; Sykes et al., 2004). Thus, for Na-dependent organic anion transport, differential sensitivity to PAH and ES would functionally map pathways of Na-dependent organic anion transport. This is one approach we have used in the present study.

The uptake of 20 μM 2,4-D into choroid plexus tissue was initially rapid, but then fell off and reached a plateau after about 10 min (Fig. 2). At steady state, the uncorrected tissue-to-medium ratio (pmol/mg tissue divided by pmol/μl medium) was about 7. Since this value substantially exceeded unity, it suggests concentrative transport. A closer examination of the early time course of 2,4-D uptake revealed that the data could be fitted with a line passing through the origin (Fig. 2, inset). The zero intercept indicates the absence of detectable binding to the tissue, a finding in agreement with the data of Nagata et al (2004) for uptake of 0.05 μM 2,4-D. The linearity of uptake indicates that measurements taken over the first 2 min approximate an initial rate. To focus on 2,4-D uptake at the apical membrane, all subsequent measurements were made under initial rate conditions.

We first probed pathways of 2,4-D uptake by examining the concentration-dependence of inhibition by PAH, ES and unlabeled 2,4-D. The basic approach was to raise the concentration of

inhibitor until its effects were maximal (reached a plateau). At that point, all uptake pathways shared by substrate and inhibitor are blocked. Incomplete inhibition indicates that more than one pathway is responsible for uptake and that the chosen inhibitor does not block them all. This approach assumes parallel, non-interacting pathways of uptake. It was used previously to define organic anion uptake pathways in choroid plexus tissue from wild-type and Oat3-null mice (Sykes et al, 2004).

Figure 3A shows that the uptake of 20 μM 2,4-D was sensitive to inhibition by PAH. Uptake was reduced in a concentration-dependent manner by PAH concentrations below 2.5 mM, but from 2.5-10 mM inhibition was constant at about 50%. We interpret these data to indicate that 2.5 mM PAH blocked all common pathways of 2,4-D uptake, but that additional pathways remained that were not sensitive to PAH.

When ES was used as inhibitor, much greater maximal inhibition was seen. With 2 mM ES, inhibition exceeded 80% (Fig. 3B). The effects of 10 mM PAH and 2 mM ES in combination were no greater than the effects of ES alone and were equivalent to those of 5 mM unlabeled 2,4-D (Fig. 4). This 2,4-D concentration is 250 times the substrate concentration; dose response experiments demonstrated that it caused maximal inhibition of 20 μM 2,4-D uptake (not shown). Together, these data define three distinct components of 2,4-D uptake: one that was sensitive to PAH and ES, a second that was sensitive to ES but not to PAH, and a third that was not affected by PAH, ES and unlabeled 2,4-D.

We characterized further the PAH-insensitive component of 20 μM 2,4-D uptake by determining whether organic anions in combination with 10 mM PAH could reduce uptake to a greater extent than 10 mM PAH alone. As shown in Fig. 5, both DHEAS and taurocholate significantly reduced the PAH-insensitive component of 2,4-D uptake. In contrast, the anionic,

neurotransmitter metabolite 5-hydroxyindole acetic acid (HIAA) was without effect. Since HIAA alone partially reduced 2,4-D uptake in the absence of PAH (Fig. 5), these data indicate HIAA only affected the PAH-sensitive component of uptake.

To determine the Na dependence of transport, tissue was preincubated in Na-free medium for 30 min and then removed to Na-free medium with 20 μM ^{3}H-2,4-D for a 2 min uptake period. Controls were maintained in Na-replete (control) medium throughout preincubation and uptake. Initial experiments indicated that 1) 30 min preincubation in control medium did not affect initial rates of 20 μM 2,4-D uptake (e.g., compare control uptake values in Figs. 2 and 3 with those in Fig. 6), and 2) the effects of Na-depletion could be reversed by a second 15 min incubation in control medium prior to the uptake period (not shown). Figure 6 shows that Na depletion had the same inhibitory effect on 2,4-D uptake as a saturating concentration of PAH. Moreover, when used in combination, 10 mM PAH and Na-depletion reduced 2,4-D uptake only slightly more than either of the treatments alone. Thus, the entire PAH sensitive component of 2,4-D uptake was Na-dependent.

Note that for Oat3 to drive organic anion uptake in a Na-dependent manner, anion exchange must be energetically coupled to Na-dicarboxylate cotransport. In this regard, using apical membrane vesicles from pig choroid plexus, Pritchard et al. (1999) demonstrated both 2,4-D/glutarate exchange and Na/glutarate cotransport. They also found glutarate stimulation of 2,4-D uptake by intact rat choroid plexus. To determine whether Na-dependent dicarboxylate uptake also occurs in intact rat choroid plexus, we measured the time course of 10 μM glutarate uptake in the presence and absence of Na. Figure 7 shows rapid initial uptake of glutarate that reached a pleateau within 30 min. At steady state the uncorrected tissue to medium ratio was nearly 20,

indicating concentrative uptake. This concentrative uptake was abolished in Na-free medium (Fig. 7).

2,4-D Efflux. Previous experiments functionally defined rat, mouse and human Oat3 as being an organic anion exchanger that is sensitive to inhibition by both PAH and ES and that can be energetically coupled to the Na gradient through organic anion-dicarboxylate exchange and Na-dicarboxylate cotransport (Sweet et al., 2002; Sweet et al., 2003). Based on inhibitor specificity and Na dependence, the PAH-sensitive component of 2,4-D uptake defined above matches this profile. If Oat3 was indeed responsible for a substantial component of 2,4-D uptake, we should also be able to demonstrate exchange of 2,4-D for other monovalent organic anions that are Oat3 substrates as well as for certain dicarboxylates. To demonstrate organic anion exchange, we preloaded choroid plexus tissue to steady state in medium containing ^{3}H-2,4-D, transferred the tissue to 2,4-D-free medium and measured efflux of label over 60 min. Figure 8A shows a representative experiment in which ^{3}H-2,4-D efflux into control medium and medium containing 1 mM unlabeled 2,4-D is plotted as a function of time. In controls, efflux was rapid and essentially complete within 60 min. It could be described by a single exponential (Fig. 8A, inset). Adding unlabeled 2,4-D to the medium accelerated efflux by a factor of about 8. Moreover, all Oat3 substrates tested significantly increased the rate of ^{3}H-2,4-D efflux (Fig. 8B). Compounds that stimulated efflux included monocarboxylates (PAH, ES and benzylpenicillin), dicarboxylates (glutarate and α-ketoglutarate) and one organic cation (cimetidine), although none of these compounds were nearly as effective as 2,4-D itself.

To determine whether 2,4-D could influence the transport of an Oat3 substrate, we measured the effects of the herbicide on the uptake and efflux of PAH. Figure 9A shows that 1-

JPET Fast Forward. Published on June 15, 2005 as DOI: 10.1124/jpet.105.087056
This article has not been copyedited and formatted. The final version may differ from this version.

100 μM 2,4-D caused concentration-dependent reductions in the initial rate of uptake of 10 μM PAH. Consistent with these findings, 1 mM 2,4-D as well as several Oat3 substrates significantly increased the rate of ^{3}H-PAH efflux from choroid plexus (Fig. 9B).

Kinetics of 2,4-D Uptake. To further characterize transport, we measured the kinetics of 2,4-D uptake. Figure 10 shows the initial rate of uptake as a function of substrate concentration over the range 0.5 to 500 μM. Clearly the rate was not a linear function of concentration, but fell off as concentration was increased. To define the nonmediated component of uptake (diffusive entry plus nonspecific accumulation), we measured uptake in the presence of a high concentration of unlabeled 2,4-D. Over a substrate concentration range of 1-100 μM, uptake in the presence of 5 mM 2,4-D was a linear function of substrate concentration; the regression line passed through the origin of the plot and had a slope of 1.04 ± 0.04 (Fig. 10, inset). Consistent with this, uptake at high 2,4-D concentrations (3-5 mM) was found to be linear; the slope of the regression line connecting these data points was 1.05 ± 0.05 (not shown).

We used this experimentally defined apparent diffusion coefficient and the data for total uptake to calculate the mediated component of uptake (Fig. 11A). A double-reciprocal plot for mediated uptake could not be fitted to a single line, indicating more than one saturable component (Fig. 11B); an Eadie-Hofstee plot of these data was also clearly non-linear (not shown). We therefore used non-linear regression to fit the data for mediated transport to a function with two Michaelis-Menten terms. The best fit (R=0.98) yielded a high affinity component with an apparent Km of 5.4 μM and a low affinity component with an apparent Km of 312 μM (Fig. 11A). The curves drawn in Figs. 10 and 11A represent the functions generated for two mediated components of uptake plus diffusion (Fig. 10; equation 1) and just the two

JPET Fast Forward. Published on June 15, 2005 as DOI: 10.1124/jpet.105.087056
This article has not been copyedited and formatted. The final version may differ from this version.

mediated components of uptake (Fig. 11A), respectively. Visually, the fit to the data points is excellent.

$$\text{Uptake} = \frac{V_{max1} * [2,4\text{-D}]}{K_{m1} + [2,4\text{-D}]} + \frac{V_{max2} * [2,4\text{-D}]}{K_{m2} + [2,4\text{-D}]} + K_D\,[2,4\text{-D}] \qquad (1)$$

We used the analytical function that describes the concentration dependence of 2,4-D uptake shown in equation (1) to calculate the contribution of each of the three components to total uptake (Fig. 12). As expected, at 20μM and below, the high affinity component accounted for well over 50% of total uptake. At about 80 μM, each of the three components contributed equally and at higher concentrations, non-mediated uptake dominated. At 20 μM 2,4-D, the model predicted 19% of total uptake to be non-mediated, 58% to be on the high affinity component and 23% to be on the low affinity component. Using the data for uptake of 20 μM 2,4-D from Figs. 3 and 4, we calculated total uptake to be partitioned as follows: non-mediated uptake, 13 ± 3% (based on inhibition by 5 mM unlabeled 2,4-D); Oat3, 52 ± 12% (based on inhibition by 10 mM PAH) or 51 ± 11% (based on Na-dependence). Thus, it appears that the Na-dependent, PAH-sensitive component of uptake that we have attributed to Oat3 matches well with the high affinity component disclosed by kinetic analysis.

DISCUSSION

In the present study, we used three approaches to reveal and characterize multiple components of 2,4-D uptake at the apical (ventricular) surface of rat choroid plexus. First, using a single substrate concentration, 20 μM, we showed that inhibition of uptake by PAH and ES saturated. For PAH, maximal inhibition was about 50 % of total uptake. For ES, maximal inhibition was about 85% of total uptake and PAH plus ES in combination was no more effective than ES alone. A blocking concentration of unlabeled 2,4-D also inhibited by about 85%. These experiments defined three components of uptake: 1) one that was not affected by millimolar concentrations of PAH, ES or unlabeled 2,4-D, 2) a second that was sensitive to inhibition by PAH and ES, and 3) a third that was sensitive to inhibition by ES but not PAH. Additional experiments showed that the third component of uptake was sensitive to inhibition by DHEAS and taurocholate, but not by HIAA.

With 20 μM 2,4-D, the major component of uptake, which was both ES- and PAH-sensitive, corresponded to the Na-dependent component of uptake. Thus, by the criteria established previously (Sweet et al., 2003), Oat3 mediated this component of uptake. It is important to note that we could not detect any component of 2,4-D uptake that was sensitive to PAH but not to ES (present study). Such a component would be indicative of transport mediated by Oat1. This was also the case when we examined the mechanisms driving PAH uptake in choroid plexus from wild-type and Oat3-null mice (Sykes et al., 2004). All mediated PAH uptake in tissue from wild-type mice was ES-sensitive and mediated uptake was abolished in tissue from Oat3-null mice. Apparently, in tissue from mouse and rat, Oat1-mediated organic anion uptake is undetectable.

Note that in the inhibition studies, millimolar PAH concentrations were needed to block uptake shared by 2,4-D and PAH. Although these concentrations may appear to be high, they reflect the low apparent Km for transport of 2,4-D on Oat3 (5 μM in present study and 10 μM from Nagata et al, (2004)) and the substantially higher apparent Ki for PAH (Ki against benzylpenicillin 398 μM (Nagata et al., 2004), but Km for uptake 67 μM (Kusuhara et al., 1999)). Assuming Michaelis-Menten kinetics, competitive inhibition, a Km for 2,4-D of 7 uM and a Ki for PAH of 250 μM (Nagata et al, 2002), one calculates that 50% inhibition of uptake mediated by Oat3 will be obtained with 960 μM PAH and 90% inhibition with nearly 8 mM PAH. Although these calculated values appear higher than those suggested by Fig 3A, they emphasize the need for high PAH concentrations in the present Oat3 blocking studies.

The second approach was based on the kinetics of 2,4-D efflux from preloaded tissue. Consistent with 2,4-D transport on Oat3, efflux from choroid plexus was accelerated by several Oat3 substrates, including, monovalent organic anions, dicarboxylates and cimetidine. Conversely, 2,4-D accelerated the efflux of the Oat3 substrate, PAH. It is noteworthy that with one exception all of the Oat3 substrates tested at millimolar concentrations at most doubled the rate of 2,4-D efflux. That exception was 2,4-D itself, which increased the rate nearly 8-fold. This finding suggests a second component of 2,4-D efflux likely on another transporter that supports organic anion exchange.

The final approach was based on analysis of the kinetics of 2,4-D uptake. As in the inhibitor studies, we found multiple components of uptake: one non-mediated and at least two mediated. Non-linear regression indicated apparent Km values of 5.4 μM and 312 μM. Because of the limitations of the kinetic approach, we cannot, by kinetic criteria alone, know whether either of the mediated components represents multiple processes with similar Km values. Of the

two discernible mediated components, the high affinity one matched the PAH-sensitive and Na-dependent component defined in inhibitor studies. That is, we found very good agreement when we compared the calculated contribution of the high affinity component to total uptake with the measured contribution of the PAH-sensitive, Na-dependent component. Thus, the high affinity component appeared to represent transport mediated by Oat3. The transporter(s) responsible for the low affinity, Na-independent component of 2,4-D uptake remains to be identified. At this point we know that 2,4-D uptake by this component is inhibited by ES, taurocholate and DHEAS. Certainly, Oatp3, which has been localized to the apical membrane of choroid plexus and which transports those organic anions (Abe et al., 1998; Kusuhara et al., 2003; Ohtsuki et al., 2003) is one candidate. However, at present, it is not known whether 2,4-D is a substrate for Oatp3.

Until recently, there was considerable uncertainty as to the transporter(s) responsible for 2,4-D uptake in choroid plexus. Uptake of 2,4-D was known to be indirectly coupled to Na (Pritchard et al., 1999) and Oat3 was shown to be both capable of Na-dependent transport (Sweet et al., 2003) and the major Na-dependent organic anion transporter at the apical side of choroid plexus epithelial cells (Nagata et al., 2002; Sweet et al., 2002; Sykes et al., 2004). However, initial experiments using a cell line that overexpressed rat Oat3 showed that 2,4-D was not transported (Hasegawa et al., 2003). More recently, Nagata et al. (2004) showed that 2,4-D was indeed a substrate for transport in the same Oat3-expressing cell line and that in rat choroid plexus the inhibitor profile and kinetics of uptake matched those of the cloned transporter. These authors also concluded that Oat3 was the only transporter responsible for 2,4-D uptake.

The present results, showing multiple mediated components of 2,4-D uptake in rat choroid plexus, are not necessarily incompatible with the data of Nagata et al. (2004). First,

Nagata et al studied the effects of inhibitors using 0.05 μM 2,4-D. At that substrate concentration, our model indicates that 87% of total uptake would be on Oat3 and only 7% on the low affinity component. The latter could easily have been too small for Nagata et al. to detect given experimental error in the inhibitor studies. Second, one can use non-linear regression to produce a highly significant fit for our data to a function with a single Michaelis-Menten term. If we had not first found from inhibitor studies that multiple mediated components contributed to 2,4-D uptake, and determined that a single Michaelis-Menten term poorly fit the data for mediated transport (non-linear Lineweaver-Burke and Eadie-Hofstee plots), we, like Nagata et al. (2004), might have concluded that a second mediated component was not needed. Clearly, experiments designed to reconcile transport in intact, native tissue with data obtained from systems expressing single, cloned transporters, require full evaluation of all aspects of transport.

Finally, as an Oat3 substrate, 2,4-D has the potential to interfere with the removal from CSF of a number of potentially toxic neurotransmitter metabolites, e.g., HIAA, indoxyl sulfate, that are themselves Oat3 substrates (Ohtsuki et al., 2002). Since the herbicide is also transported by a second organic anion transporter, albeit with substantially lower affinity, it may also alter the removal of additional compounds that are handled by the second transporter. Molecular identification of the Na-independent transporter involved is likely to expand the list of possible competitive interactions.

REFERENCES

Abe T, Kakyo M, Sakagami H, Tokui T, Nishio T, Tanemoto M, Nomura H, Hebert SC, Matsuno S, Kondo H and Yawo H (1998) Molecular characterization and tissue distribution of a new organic anion transporter subtype (oatp3) that transports thyroid hormones and taurocholate and comparison with oatp2. *J Biol Chem* **273**:22395-22401.

Breen CM, Sykes DB, Baehr C, Fricker G and Miller DS (2004) Fluorescein-Methotrexate Transport in Rat Choroid Plexus Analyzed Using Confocal Microscopy. *Am J Physiol Renal Physiol*.

Breen CM, Sykes DB, Fricker G and Miller DS (2002) Confocal imaging of organic anion transport in intact rat choroid plexus. *Am J Physiol Renal Physiol* **282**:F877-885.

Choudhuri S, Cherrington NJ, Li N and Klaassen CD (2003) Constitutive expression of various xenobiotic and endobiotic transporter mRNAs in the choroid plexus of rats. *Drug Metab Dispos* **31**:1337-1345.

Ghersi-Egea JF and Strazielle N (2002) Choroid plexus transporters for drugs and other xenobiotics. *J Drug Target* **10**:353-357.

Hasegawa M, Kusuhara H, Endou H and Sugiyama Y (2003) Contribution of organic anion transporters to the renal uptake of anionic compounds and nucleoside derivatives in rat. *J Pharmacol Exp Ther* **305**:1087-1097.

Kim CS and O'Tuama LA (1981) Choroid plexus transport of 2,4-dichlorophenoxyacetic acid: interaction with the organic acid carrier. *Brain Res* **224**:209-212.

Kusuhara H, He Z, Nagata Y, Nozaki Y, Ito T, Masuda H, Meier PJ, Abe T and Sugiyama Y (2003) Expression and functional involvement of organic anion transporting polypeptide subtype 3 (Slc21a7) in rat choroid plexus. *Pharm Res* **20**:720-727.

Kusuhara H, Sekine T, Utsunomiya-Tate N, Tsuda M, Kojima R, Cha SH, Sugiyama Y, Kanai Y and Endou H (1999) Molecular cloning and characterization of a new multispecific organic anion transporter from rat brain. *J Biol Chem* **274**:13675-13680.

Kusuhara H and Sugiyama Y (2004) Efflux transport systems for organic anions and cations at the blood-CSF barrier. *Adv Drug Deliv Rev* **56**:1741-1763.

Leggas M, Adachi M, Scheffer GL, Sun D, Wielinga P, Du G, Mercer KE, Zhuang Y, Panetta JC, Johnston B, Scheper RJ, Stewart CF and Schuetz JD (2004) Mrp4 confers resistance to topotecan and protects the brain from chemotherapy. *Mol Cell Biol* **24**:7612-7621.

Miller DS (2004) Confocal imaging of xenobiotic transport across the choroid plexus. *Adv Drug Deliv Rev* **56**:1811-1824.

Nagata Y, Kusuhara H, Endou H and Sugiyama Y (2002) Expression and functional characterization of rat organic anion transporter 3 (rOat3) in the choroid plexus. *Mol Pharmacol* **61**:982-988.

Nagata Y, Kusuhara H, Imaoka T, Endou H and Sugiyama Y (2004) Involvement of rat organic anion transporter 3 in the uptake of an organic herbicide, 2,4-dichlorophenoxyacetate, by the isolated rat choroid plexus. *J Pharm Sci* **93**:2724-2732.

Ohtsuki S, Asaba H, Takanaga H, Deguchi T, Hosoya K, Otagiri M and Terasaki T (2002) Role of blood-brain barrier organic anion transporter 3 (OAT3) in the efflux of indoxyl sulfate, a uremic toxin: its involvement in neurotransmitter metabolite clearance from the brain. *J Neurochem* **83**:57-66.

Ohtsuki S, Takizawa T, Takanaga H, Terasaki N, Kitazawa T, Sasaki M, Abe T, Hosoya K and Terasaki T (2003) In vitro study of the functional expression of organic anion

transporting polypeptide 3 at rat choroid plexus epithelial cells and its involvement in the cerebrospinal fluid-to-blood transport of estrone-3-sulfate. *Mol Pharmacol* **63**:532-537.

Pappenheimer JR, Heisey SR and Jordan EF (1961) Active transport of Diodrast and phenolsulfonphthalein from cerebrospinal fluid to blood. *Am J Physiol* **200**:1-10.

Pritchard JB (1980) Accumulation of anionic pesticides by rabbit choroid plexus in vitro. *J Pharmacol Exp Ther* **212**:354-359.

Pritchard JB and Miller DS (1993) Mechanisms mediating renal secretion of organic anions and cations. *Physiol Rev* **73**:765-796.

Pritchard JB, Sweet DH, Miller DS and Walden R (1999) Mechanism of organic anion transport across the apical membrane of choroid plexus. *J Biol Chem* **274**:33382-33387.

Sweet DH, Chan LM, Walden R, Yang XP, Miller DS and Pritchard JB (2003) Organic anion transporter 3 (Slc22a8) is a dicarboxylate exchanger indirectly coupled to the Na+ gradient. *Am J Physiol Renal Physiol* **284**:F763-769.

Sweet DH, Miller DS, Pritchard JB, Fujiwara Y, Beier DR and Nigam SK (2002) Impaired organic anion transport in kidney and choroid plexus of organic anion transporter 3 (Oat3 (Slc22a8)) knockout mice. *J Biol Chem* **277**:26934-26943.

Sykes D, Sweet DH, Lowes S, Nigam SK, Pritchard JB and Miller DS (2004) Organic anion transport in choroid plexus from wild-type and organic anion transporter 3 (Slc22a8)-null mice. *Am J Physiol Renal Physiol* **286**:F972-978.

Villalobos AR, Miller DS and Renfro JL (2002) Transepithelial organic anion transport by shark choroid plexus. *Am J Physiol Regul Integr Comp Physiol* **282**:R1308-1316.

Wijnholds J, deLange EC, Scheffer GL, van den Berg DJ, Mol CA, van der Valk M, Schinkel AH, Scheper RJ, Breimer DD and Borst P (2000) Multidrug resistance protein 1 protects

the choroid plexus epithelium and contributes to the blood-cerebrospinal fluid barrier. *J Clin Invest* **105**:279-285.

FIGURE LEGENDS

Figure 1. Organic anion transporters in choroid plexus. The diagram shows transporters with known subcellular locations, based on specific immunostaining for transporter protein (Ghersi-Egea and Strazielle, 2002; Kusuhara and Sugiyama, 2004; Leggas et al., 2004; Miller, 2004).

Figure 2. Time course of 2,4-D uptake. Tissue was incubated in aCSF with 20 μM ^{3}H-2,4-D for the indicated time and then weighed and processed for liquid scintillation counting. Inset shows uptake over the first 2 min of incubation. Linear regression demonstrated that the y-intercept was not significantly different from zero; The regression line drawn was forced through the origin. Each point represents the mean value for tissue from 3-6 rats; variability is given as SE bars.

Figure 3. Effects of p-aminohippurate (PAH) and estrone sulfate (ES) on uptake of 2,4-D. Tissue was incubated in aCSF with 20 μM ^{3}H-2,4-D and the indicated concentration of PAH (A) or ES (B) for 2 min and then weighed and processed for liquid scintillation counting. Each point represents the mean value for tissue from 3-9 rats; variability is given as SE bars. Statistical comparisons: Significantly reduced uptake ($P<0.01$ compared to controls) was found with PAH concentrations ≤0.1 mM and ES concentrations ≤50 μM.

Figure 4. Inhibition of 2,4-D uptake by saturating concentrations of p-aminohippurate (PAH), estrone sulfate (ES) and 2,4-D. Tissue was incubated in aCSF for 2 min with 20 μM ^{3}H-2,4-D without (control) or with the indicated concentration of inhibitor and then weighed and processed for liquid scintillation counting. Each point represents the mean value for tissue from 3-6 rats; variability is given as SE bars. ** Significantly lower than controls, $P<0.01$.

Figure 5. Inhibition of the PAH-insensitive component of 2,4-D uptake by organic anions. Tissue was incubated in aCSF for 2 min with 20 μM ^{3}H-2,4-D without (control) or with the indicated concentration of inhibitor and then weighed and processed for liquid scintillation counting. Each point represents the mean value for tissue from 3-12 rats; variability is given as SE bars. 5HIAA, 5-hydroxyindole acetic acid; TC, taurocholate. All treatments tested significantly reduced 2,4-D uptake below control values ($P<0.01$). ** Significantly lower than 10 mM PAH alone ($P<0.01$).

Figure 6. Na dependence of 2,4-D uptake. Tissue was preincubated in aCSF or Na-free CSF for 15 min, removed to aCSF or Na-free aCSF for a 2 min incubation with 20 μM ^{3}H-2,4-D without (control) or with p-aminohippurate (PAH) and then weighed and processed for liquid scintillation counting. Each point represents the mean value for tissue from 3-6 rats; variability is given as SE bars. ** Significantly lower than controls, $P<0.01$.

Figure 7. Time course of glutarate uptake. Tissue was incubated in aCSF or Na-free aCSF with 10 μM ^{3}H-glutarate for the indicated time and then weighed and processed for liquid scintillation counting. Each point represents the mean value for tissue from 3-6 rats; variability is given as SE bars. At all times, uptake in Na-free medium was significantly lower than controls ($P<0.01$).

Figure 8. Efflux of 2,4-D from preloaded choroid plexus. Tissue was loaded in aCSF containing 20 μM ^{3}H-2,4-D, transferred to label-free aCSF without (control) and with the indicated additions. (A) Time course of efflux into control aCSF and aCSF containing 1 mM unlabeled 2,4-D. The inset shows that semilog plots of the data are linear, indicating first-order kinetics. (B) First order rate constants for 2,4-D efflux into aCSF containing the

indicated additions. Shown are mean values for tissue from 3-12 rats; variability is given as SE bars. ** Significantly greater than controls ($P<0.01$).

Figure 9. Effects of organic anions on PAH uptake (A) and efflux (B). For uptake measurements, tissue was incubated for 2 min in aCSF with 10 μM ^{3}H-PAH and the indicated concentration of 2,4-D. For efflux measurements, tissue was loaded in aCSF containing 10 μM ^{3}H-PAH, transferred to label-free aCSF without (control) and with the indicated organic anions. For each treatment, semilog plots of fraction label remaining vs time were linear. First order rate constants were calculated from these data using non-linear regression. Data given as mean value for tissue from 3-9 rats; variability is shown as SE bars. * Significantly greater than controls ($P<0.05$); ** significantly greater than controls ($P<0.01$).

Figure 10. Concentration dependence of 2,4-D uptake. Tissue was incubated for 2 min in aCSF with the indicated concentration of ^{3}H-2,4-D and then weighed and processed for liquid scintillation counting. The curve was generated from equation (1). Inset shows that uptake from aCSF containing 5 mM unlabeled 2,4-D is a linear function of ^{3}H-2,4-D concentration, thus defining the uptake vs concentration relationship for non-mediated transport. Each point represents the mean value for tissue from 6 rats; variability is given as SE bars.

Figure 11. Mediated uptake of 2,4-D. (A) Concentration dependence of mediated uptake (obtained by subtracting calculated non-mediated uptake from total uptake at each concentration, see text). The constants shown were obtained from non-linear regression of the data using a model with 2 Michaelis-Menten terms; the curve is a plot of that

function. (B) Non-linear Lineweaver-Burke plot, indicating multiple mediated components of uptake.

Figure 12. Contribution of each of the three components to total uptake calculated from equation (1) using the kinetic constants shown in Fig. 11A and the apparent diffusion coefficient derived from the data in the inset to Fig. 10. Values are given as fraction of total uptake in each component.

Fig. 1

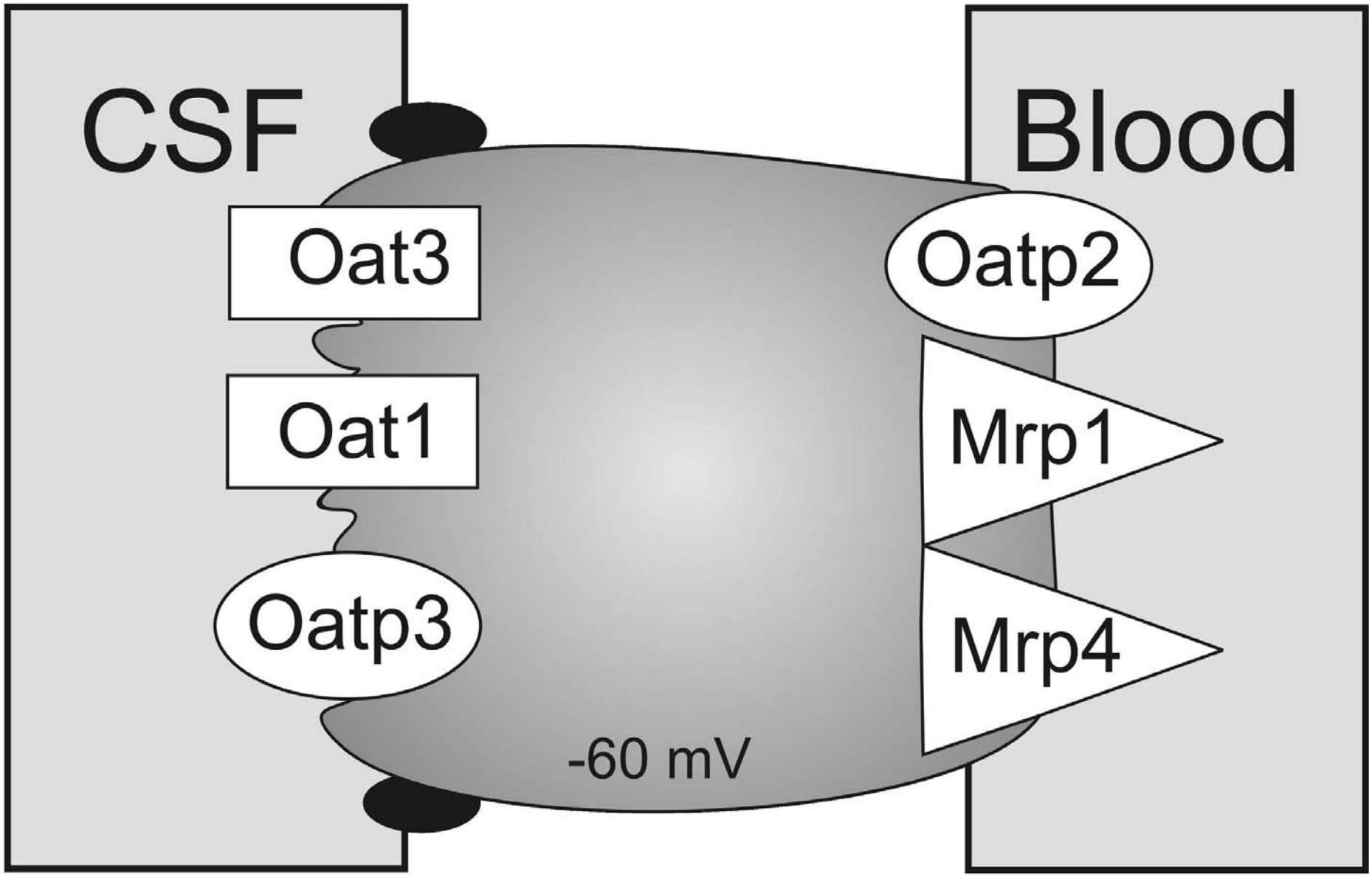

JPET Fast Forward. Published on June 15, 2005 as DOI: 10.1124/jpet.105.087056
This article has not been copyedited and formatted. The final version may differ from this version.

Fig. 2

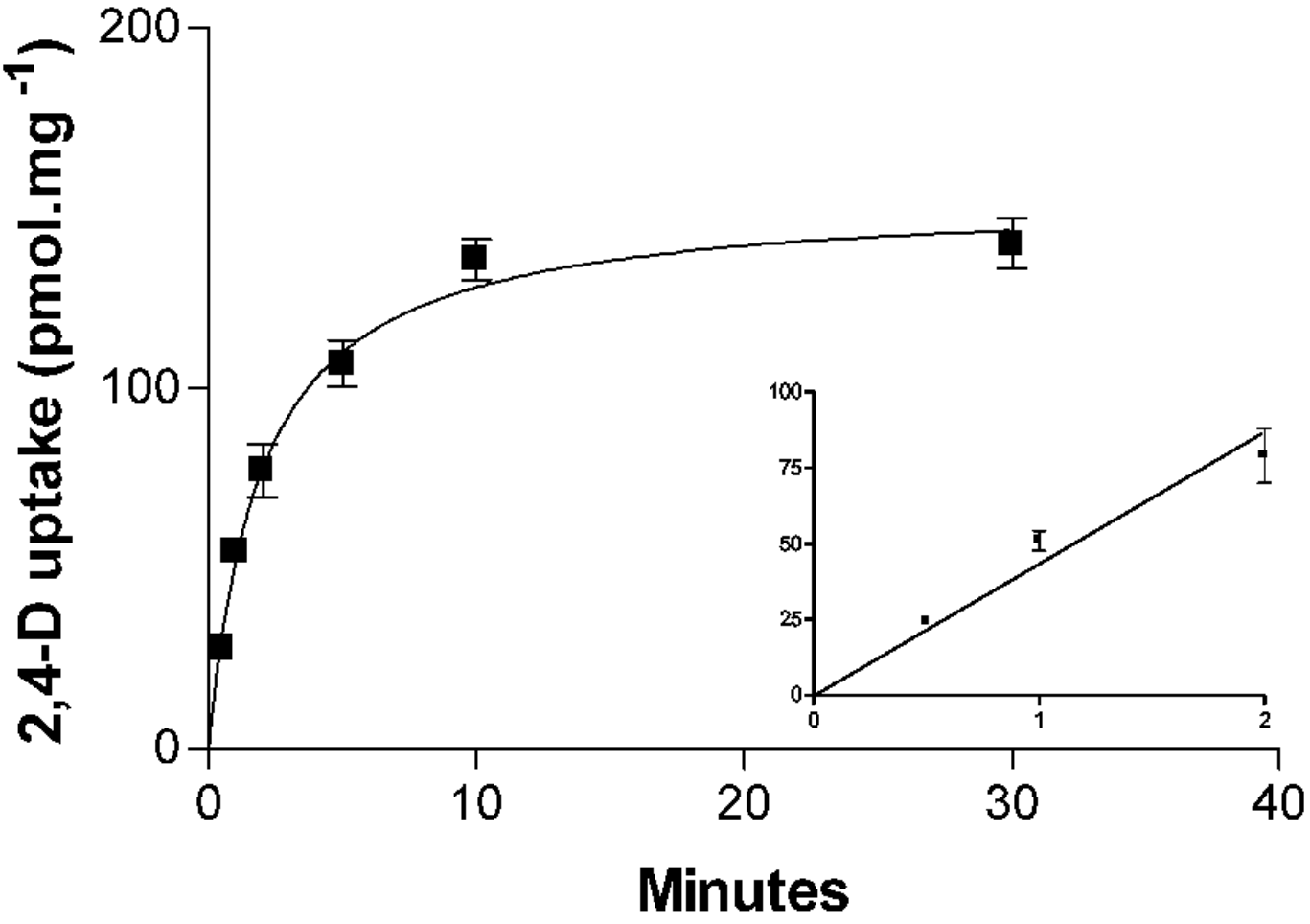

JPET Fast Forward. Published on June 15, 2005 as DOI: 10.1124/jpet.105.087056
This article has not been copyedited and formatted. The final version may differ from this version.

Fig. 3

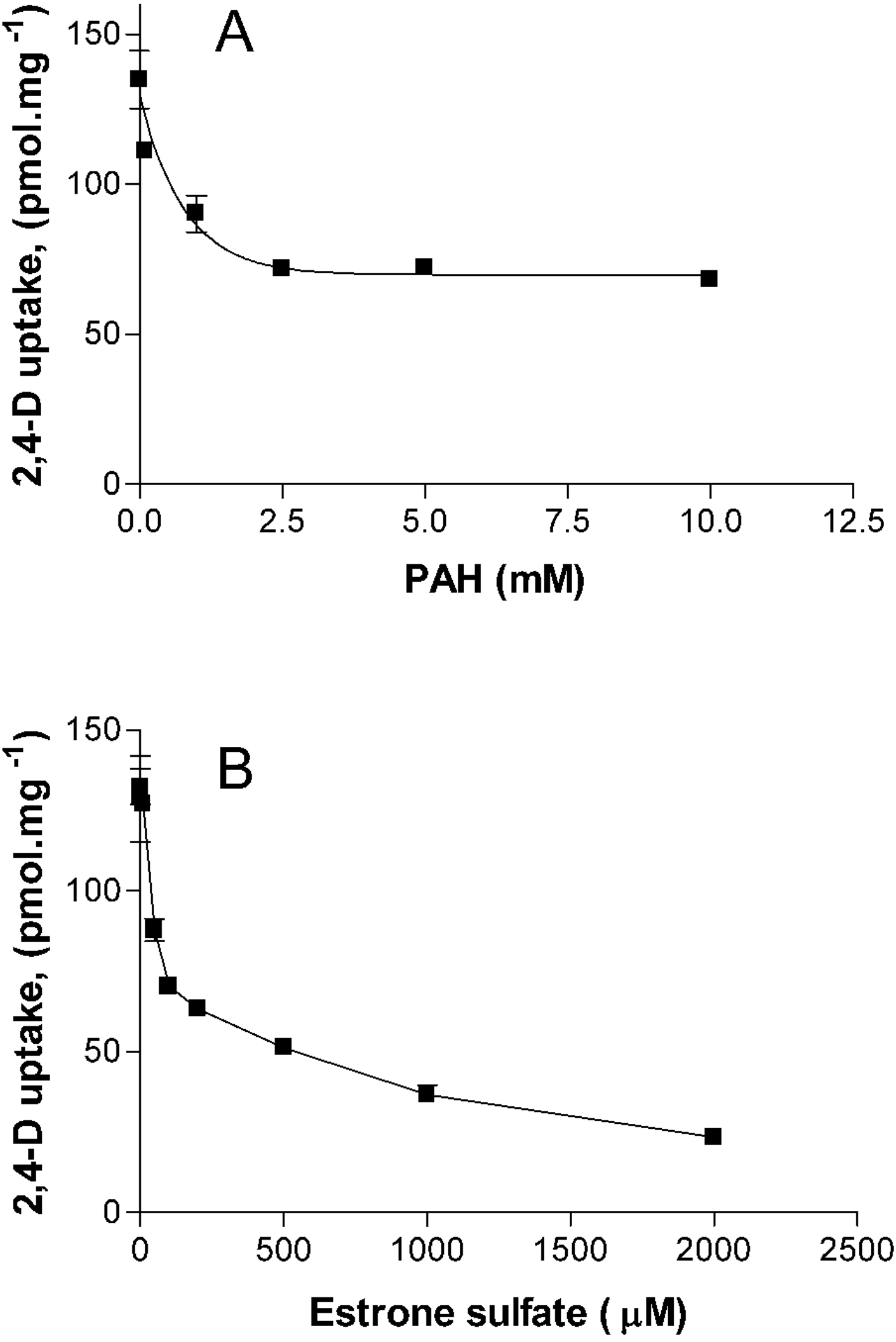

JPET Fast Forward. Published on June 15, 2005 as DOI: 10.1124/jpet.105.087056
This article has not been copyedited and formatted. The final version may differ from this version.

Fig. 4

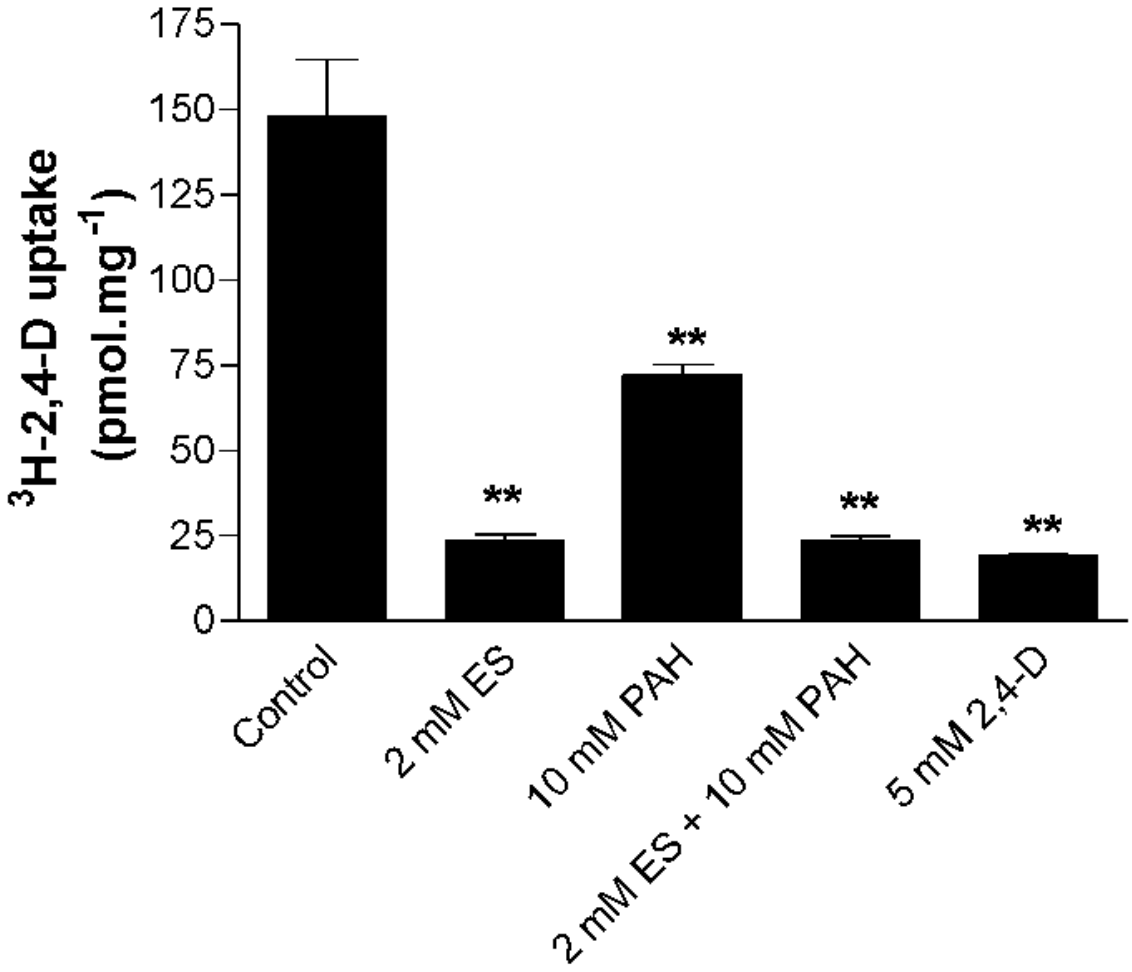

JPET Fast Forward. Published on June 15, 2005 as DOI: 10.1124/jpet.105.087056
This article has not been copyedited and formatted. The final version may differ from this version.

Fig. 5

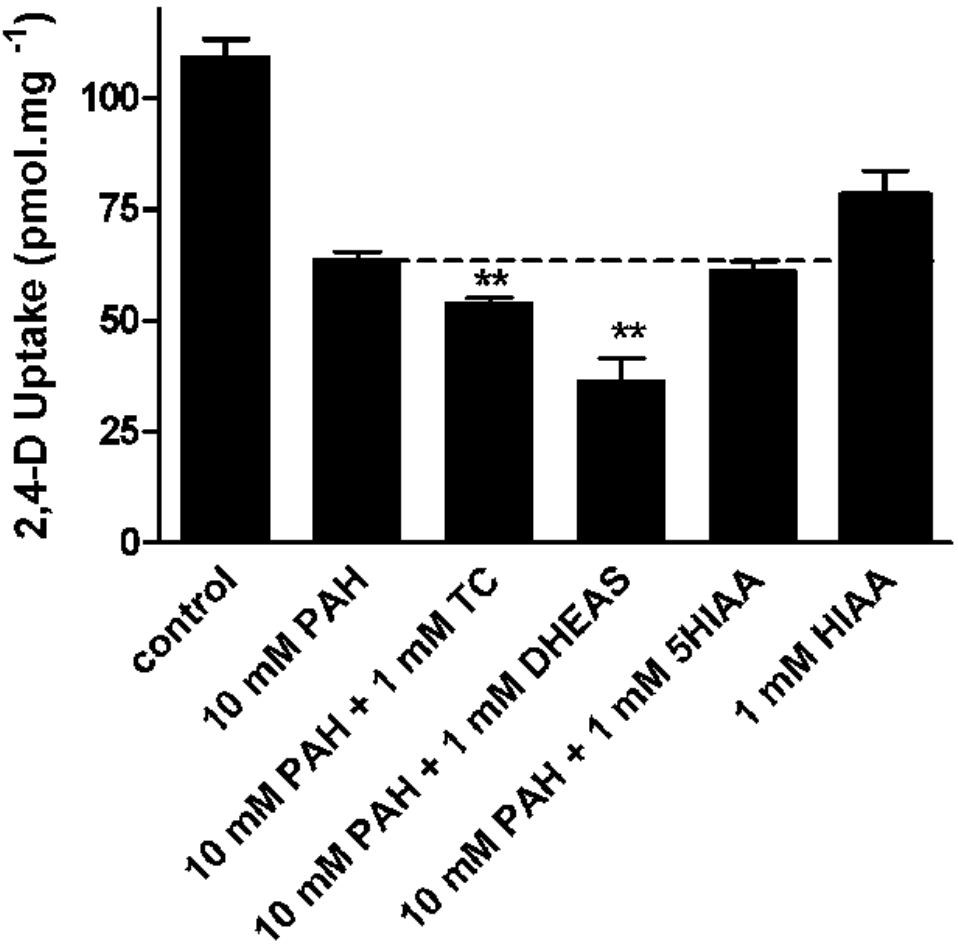

JPET Fast Forward. Published on June 15, 2005 as DOI: 10.1124/jpet.105.087056
This article has not been copyedited and formatted. The final version may differ from this version.

Fig. 6

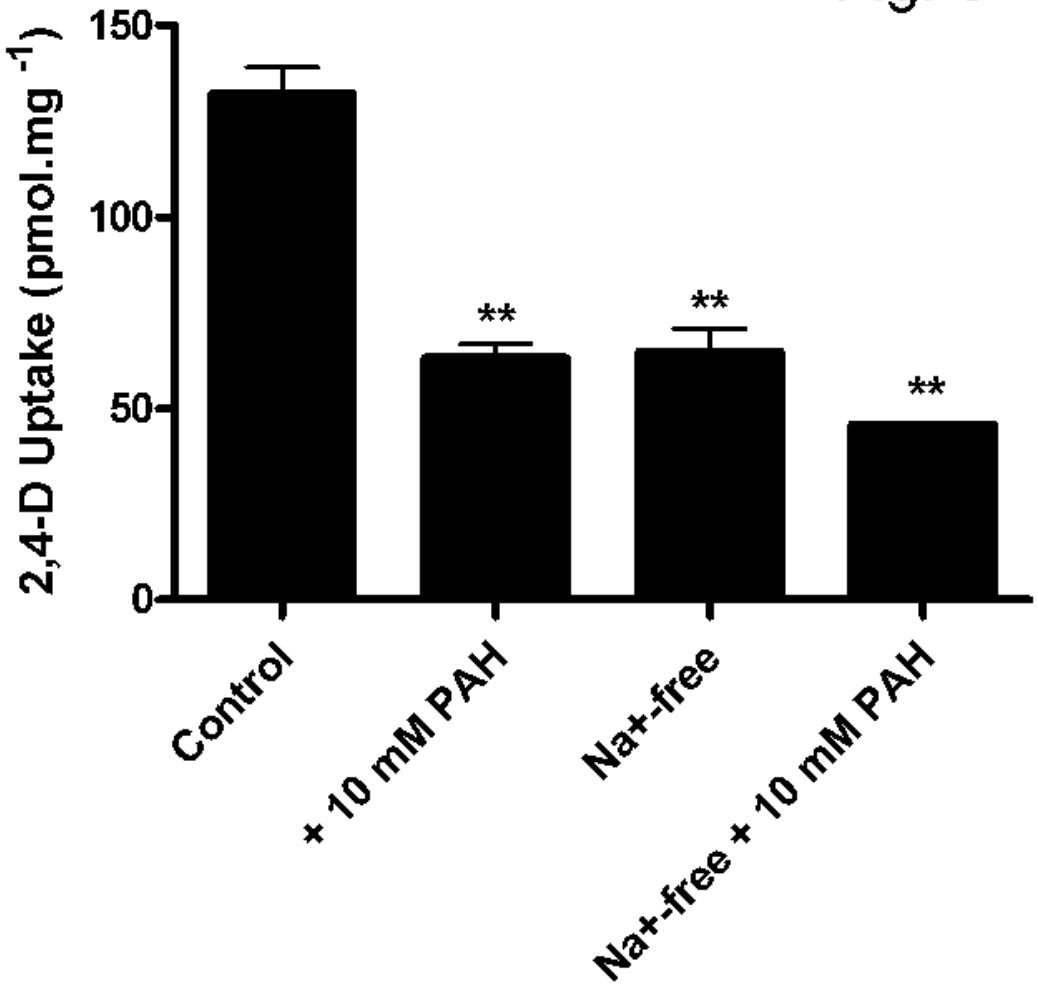

JPET Fast Forward. Published on June 15, 2005 as DOI: 10.1124/jpet.105.087056
This article has not been copyedited and formatted. The final version may differ from this version.

Fig. 7

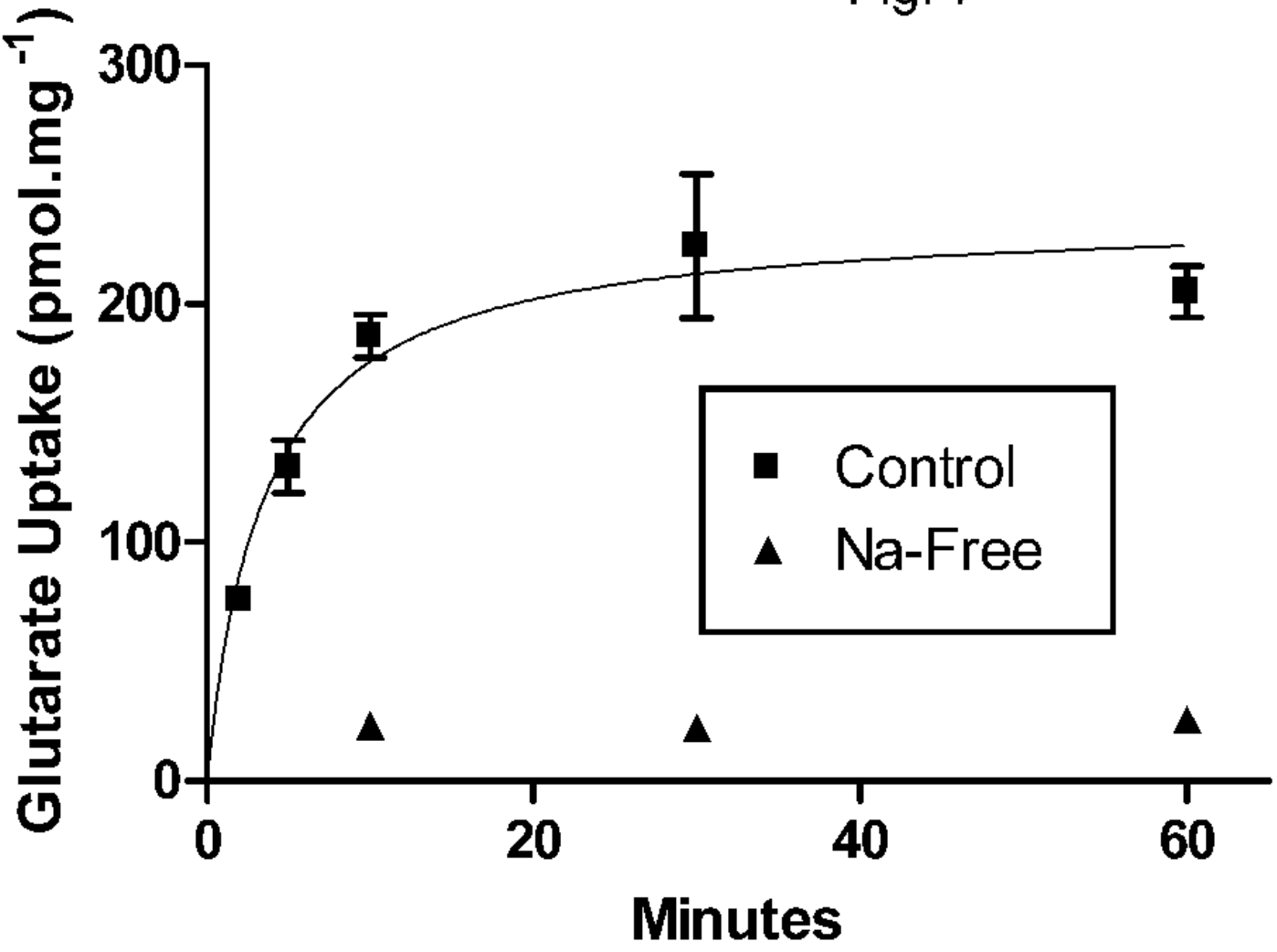

JPET Fast Forward. Published on June 15, 2005 as DOI: 10.1124/jpet.105.087056
This article has not been copyedited and formatted. The final version may differ from this version.

Fig. 8

A

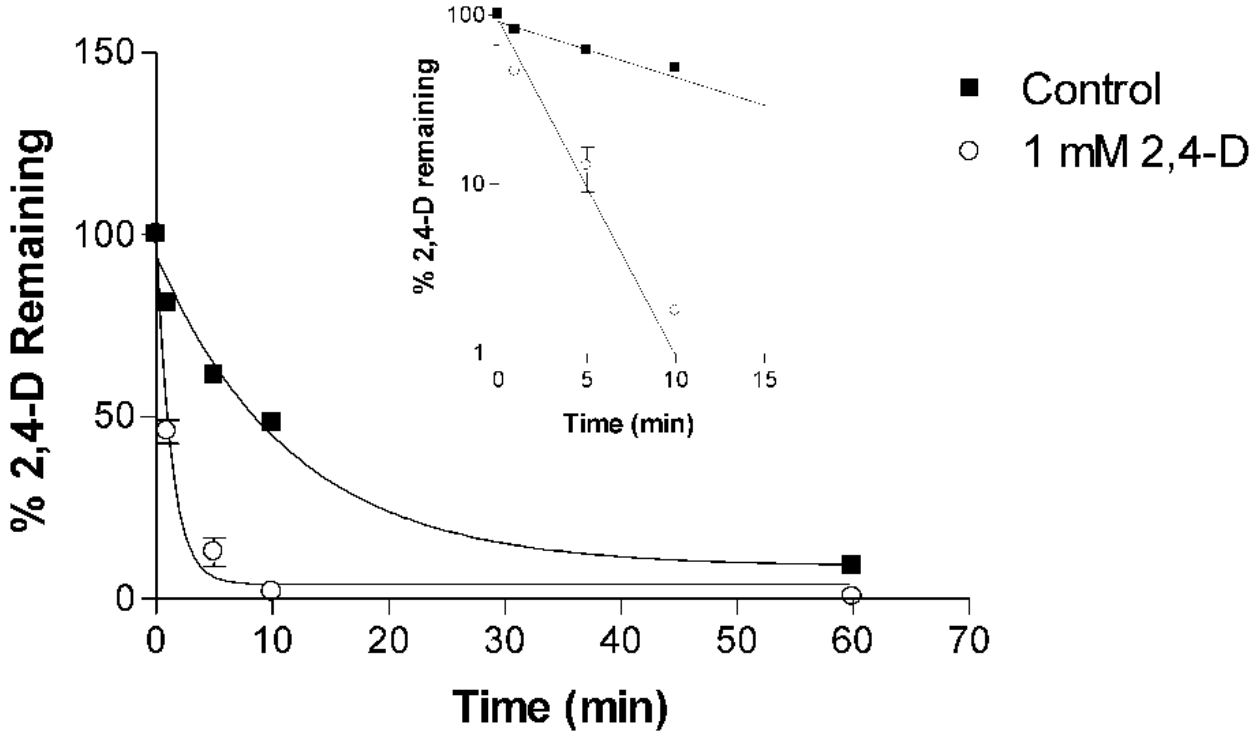

B

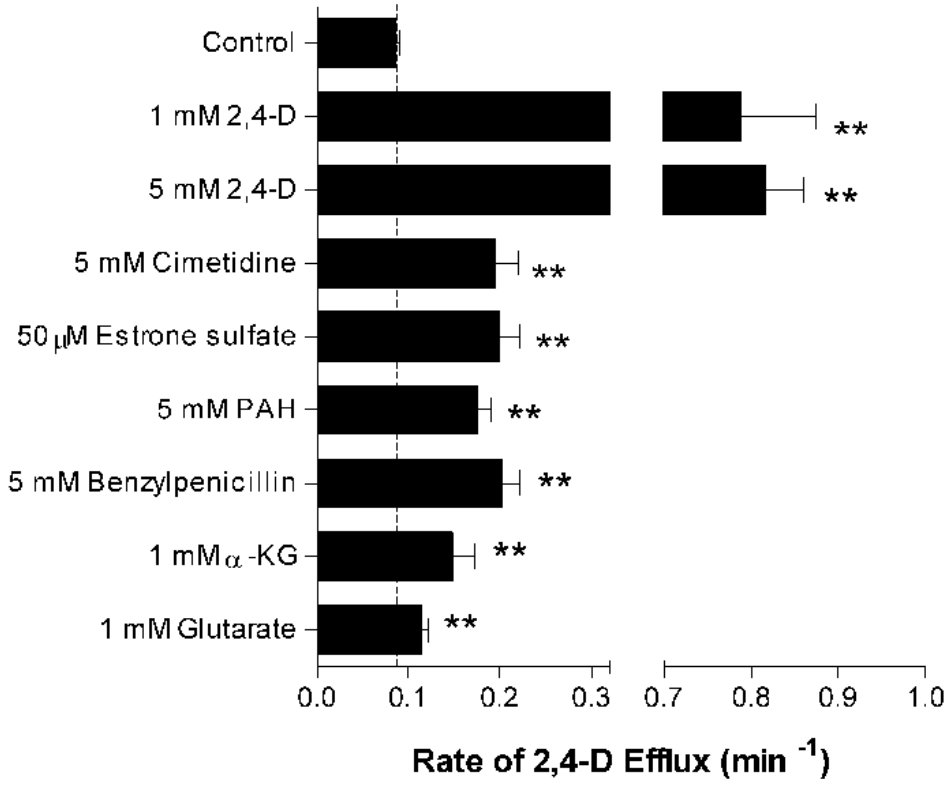

JPET Fast Forward. Published on June 15, 2005 as DOI: 10.1124/jpet.105.087056
This article has not been copyedited and formatted. The final version may differ from this version.

Fig. 9

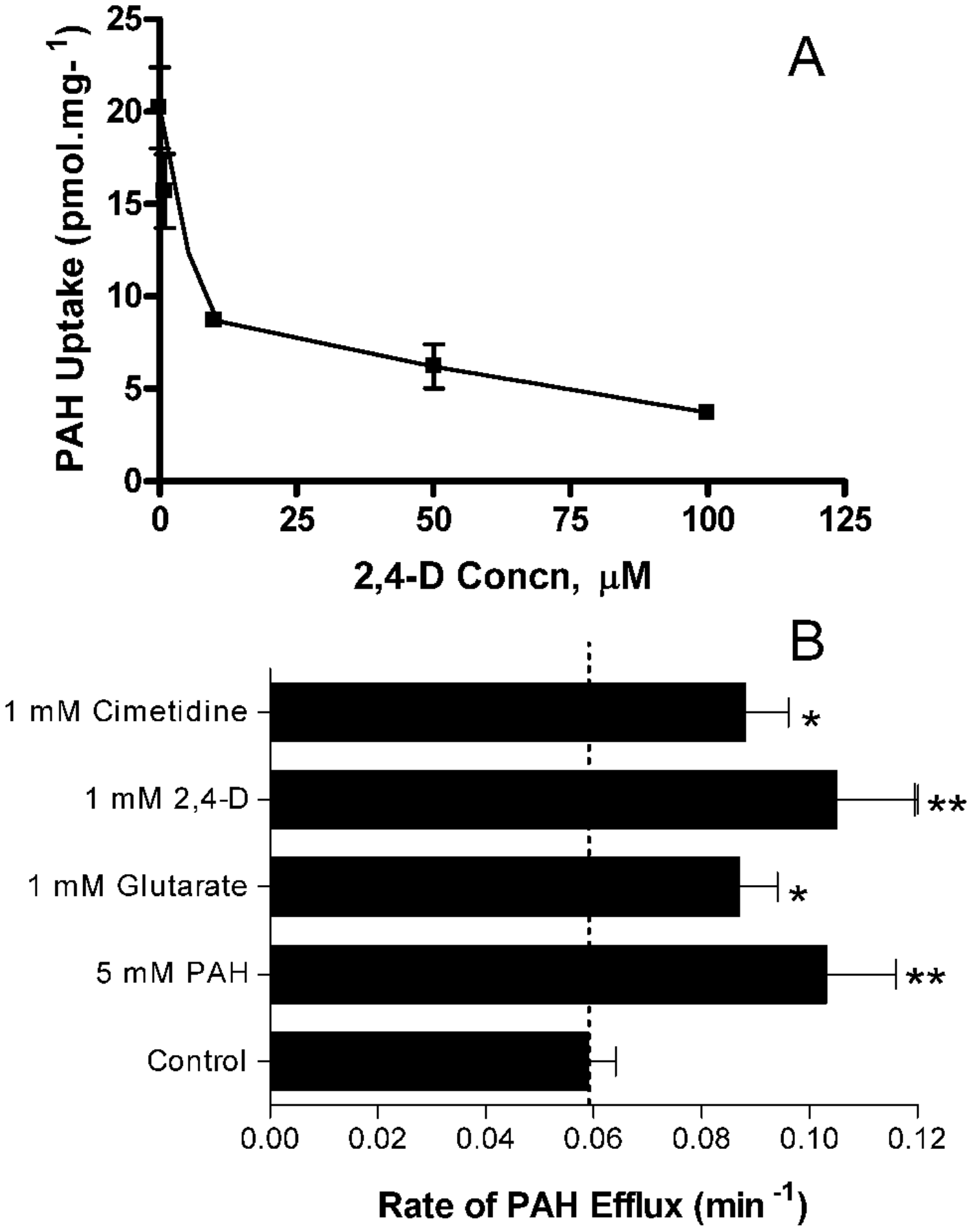

JPET Fast Forward. Published on June 15, 2005 as DOI: 10.1124/jpet.105.087056
This article has not been copyedited and formatted. The final version may differ from this version.

Fig. 10

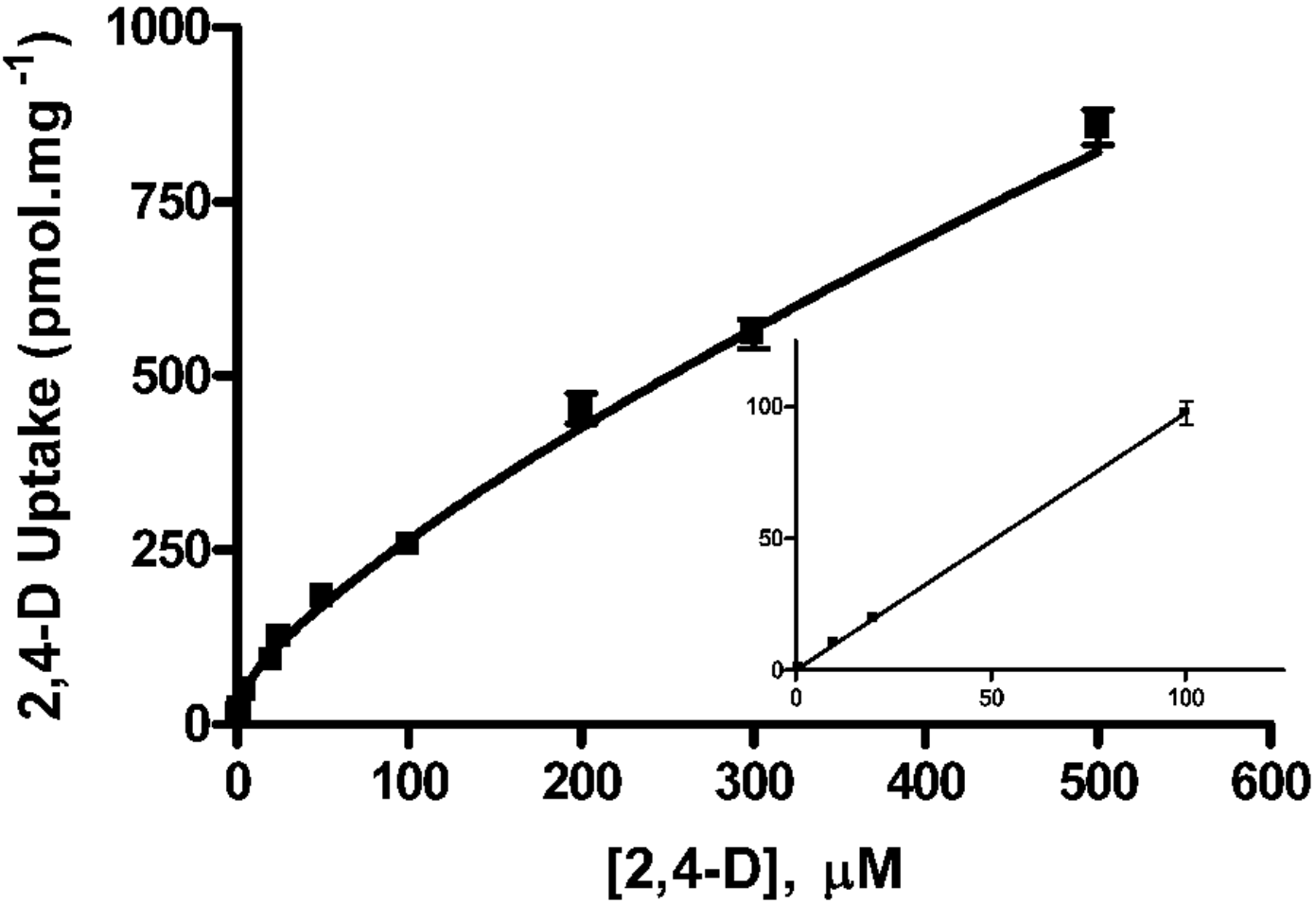

JPET Fast Forward. Published on June 15, 2005 as DOI: 10.1124/jpet.105.087056
This article has not been copyedited and formatted. The final version may differ from this version.

Fig. 11

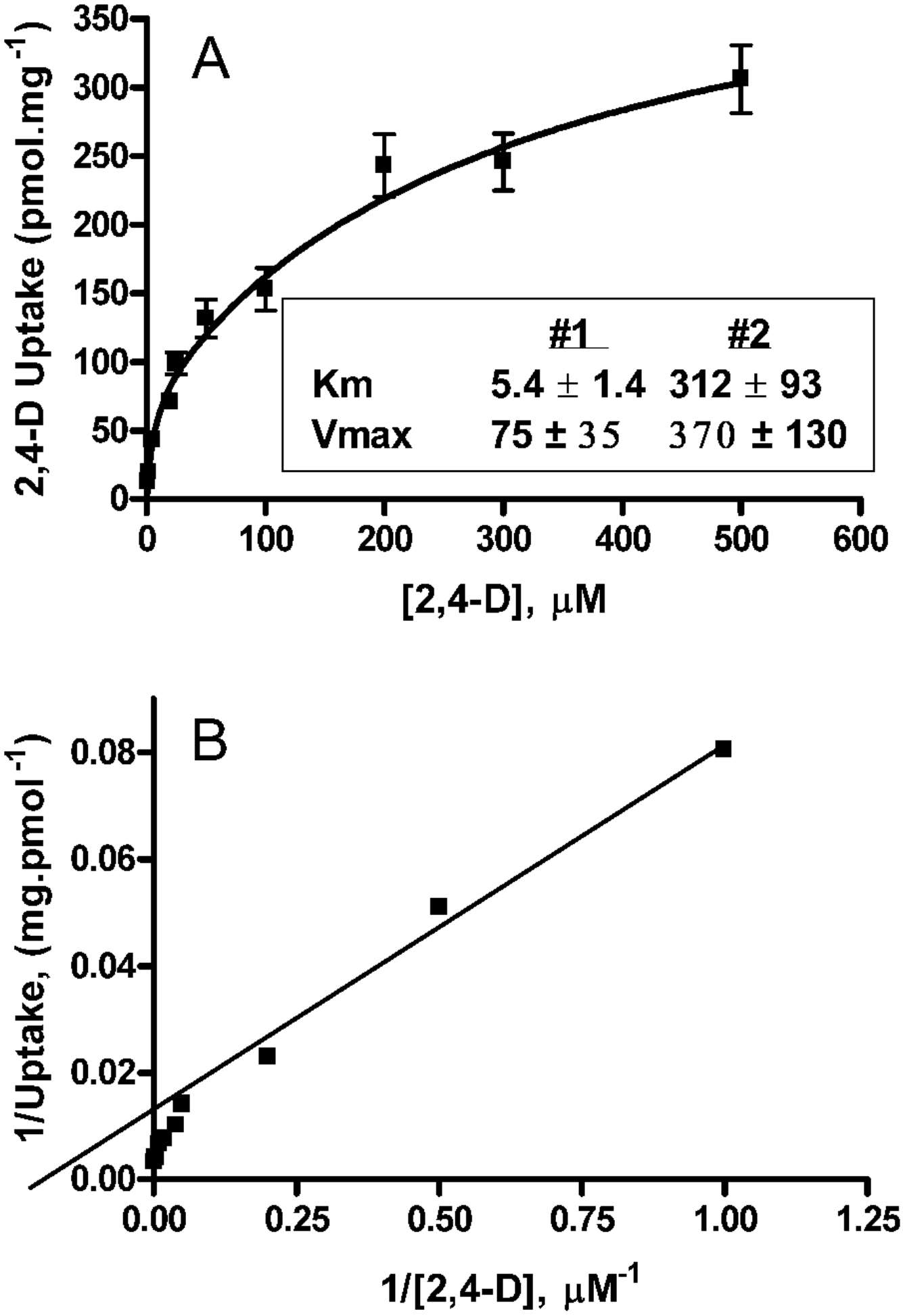

JPET Fast Forward. Published on June 15, 2005 as DOI: 10.1124/jpet.105.087056
This article has not been copyedited and formatted. The final version may differ from this version.

Fig. 12